SUPPLEMENTAL MATERIALS AND METHODS

Circumferential Radioluminescence Imaging (CRI) Peripheral System Design

The components of CIRPI system is described in our previously published study[26]. In brief, the optical components of the CIRPI system consists of a 10x magnification infinity-corrected microscope objective (RMS10x, Olympus Inc.) with a working distance of 10.6 mm, numerical aperture (NA) of 0.25 and effective focal length (EFL) of 18 mm (Supplemental Fig. 1). The system also contains an infinity-corrected tube lens for plan fluorite objective (ITL200, Thorlabs) in between the objective (F2 = 102 mm) and the ProEM charge-coupled device (CCD) camera (F3 = 200 mm) (Princeton Instruments). The CIRPI system provides a 360˚ view inside an artery through an innovative probe design (see section on Dual-Modality Endoscopic Probe).

The novelty of this CIRPI system is based on a scintillating window made from organic calcium fluoride doped with europium (CaF_2:Eu) phosphor, placed on the catheter-based probe to convert the β-particles of the positron emission signal into visible light due to radioactive decay (primary decay time 940 ns). The molecules in the scintillating window get excited with the incoming ionizing radiation, especially β-particles from the decay of ^{18}F-FDG, or other isotopes, by absorbing energy. When these molecules return to a lower energy state from an excited state, they release optical radiation in the visible range. This light is then captured with a *highly sensitive* CCD camera using deep thermoelectric cooling at -70°C for minimizing the background signal from the temperature-dependent dark current, hot pixel blemishes, and vibration. The deep thermoelectric cooling was done with a CoolCUBE II liquid circulatory system. The camera exposure times were set to 45 seconds based on sensitivity (above this threshold the pixels were saturated). For ^{18}F-FDG imaging with the CIRPI system, the binning factor was set at smallest limit (1x1 pixel) with effective active imaging resolutions of 1024 x

1024 pixels (width x height). The analog-to-digital conversion speed was set to 10 MHz with corresponding EM gain of 50 at 16-bits bit depth. The storage shift rate was set to 600 ns with readout time of 4 ms for 'frame transfer' readout mode. The CCD camera shutter mode was set to "always open" without any delay (0 ms) in opening and closing. The selection process of optimal scintillating material and resolution were described in the our previously published manuscript [25].

Photoacoustic Tomography (PAT) Peripheral System Design

The PAT peripheral system has re-designed to perform faster data acquisition from our previously published study.[24] For PAT system, we used a tunable Horizon I OPO pumped by Surelite II nanosecond laser (192-2750 nm Continiuum, San Jose, CA, USA) with 4-7 mm beam diameter (before focusing into the 200 µm core multimode fiber). The peak wavelength of the laser's spectral bandwidth can be tuned to multiple values for selective imaging of the different tissue constituents. The central hypothesis of this PAT imaging is that the absorption spectra of calcium, lipids, elastic, and collagen are sufficiently well differentiated from those of the constituents of normal arterial tissue in the 500 to 1400 nm wavelength range to permit the detection of calcium or lipid-rich plaques using PAT imaging.

The repetition rate was set to the highest at 20 Hz with 3-5 ns FWHM pulse length. The laser was linearly polarized at <2 mrad divergence. The Horizon tunable laser operates at 110 V and is connected to Surelite 210. Power supply for Surelite 210 operates at 220 V and attached to a coolant circulation to regulate the temperature. Horizon sends an Sync Out signal as an external trigger to a pulse-receiver signal generator (5073PR-15U, 75 MHz Bandwidth, 39dB, RF Gain, 115 VAC Olympus America Inc., Waltham, MA, USA). A pre-amplifier receives the PA signal from the multi-mode

optical probe and after 8× amplification this signal is sent to pulser-receiver. This 75 MHz computer controlled pulser-receiver is used to trigger a four-channel, 14-bit Digital Acquisition System (NI PXIe-5170R, 250 MS/s, 100 MHz, Oscilloscope with 750 MB RAM and Kintex-7 325T FPGA, NI, USA) and receive the amplified PA signal. A custom written Matlab code was used to concatenate 330 A-lines captured during a 360˚ rotation to generate a B-scan.

Dual-Modality Endoscopic Probe

The components of CIRPI system probe is described in our previously published study[26]. However, the probe is reduced in diameter. The CIRPI system includes a novel optical probe combining circumferential radioluminescence imaging (CRI) and photoacoustic tomography (PAT) (Supplemental Fig. 2A). The probe's CaF_2:Eu-based scintillating imaging window captures radioluminescence images (360˚ view) of plaques by converting β-particles to visible photons during ^{18}F-FDG decay (Supplemental Fig. 2B). A single 360º arterial radioluminescence image acquisition is 45 seconds for our CIRPI system. During radioluminescence imaging, the visible photons from optical radiation of high energy β-particles reflect to/from the 45º scanning mirror. These photons were then collected through the GRIN lens followed by creating a 18,000 pixels image at every 1.43º rotation of the mirror. A total of 63 images were collected for each quadrant of the circular arterial wall. A tunable laser-based PAT characterizes tissue constituents of plaque at 7 different wavelengths—540-560 nm (calcification), 920 nm (cholesteryl ester), 1040 nm (phospholipids), 1180 nm (elastin/collagen), 1210 nm (cholesterol), and 1235 nm (triglyceride) (Supplemental Fig. 2C).

The CIRPI probe (Supplemental Figs. 2D, 2E) has a 840 mm flexible tether with up to 17˚ of bending freedom and a 36 mm (previously 42 mm) long rigid distal imaging

head consists of (1) a CaF_2:Eu scintillating imaging window, (2) a light guiding multi-mode optical fiber (OF-1, 0.22 NA, 0.2 mm core diameter; Thorlabs Inc., USA), (3) a leached image fiber (OF-2, 18,000 optical fibers represent a 0.9 mm diameter imaging area with 7.4 μm pixel size; Schott Inc., USA), (4) a single-element ultrasonic transducer (Lithium Niobate LNO, 40 MHz, unfocused, ring transducer with OD = 2 mm, ID = 1.37 mm, and length of 5.1 mm), (5) a digital actuator (2.0 mm diameter, 18.62 mm long; Namiki Precision Jewel Co., Ltd. Japan), and (6) 45˚ degree flat rotating mirror (2 mm diameter, protected aluminum on glass substrate, with the reflection surface at 45° to the probe's axis; Edmund Optics Inc., USA) that was placed in a stainless steel tube housing. The absolute field-of-view of 0.9 mm imaging area is 6.5 mm. A single-element ultrasonic transducer was used for achieving a high Signal to Noise Ratio (SNR) at MHz repetition rates. Laser pulses from a portable UV-VIS-NIR tunable laser (7 ns pulse length at 20 Hz repetition rate) were coupled into a multimode fiber using a 10x microscope objective. These laser pulses are guided by the multi-mode optical fiber which is also positioned parallel to an imaging fiber-bundle belonging to the CIRPI system. These pulses are then emitted into the tissue through a central hole (1.37 mm diameter) in the transducer located in the distal end of the probe. The distal end of the OF-2 was terminated by a 1 mm diameter Gradient-Index (GRIN) lens designed to have a working distance of 5 mm, and paraxial magnification of 5.86. The GRIN lens provides an NA of 0.5, and radial index gradient has a maximum central refractive index of 1.635 at the lens axis.

The scintillating window was fabricated from a polymer based polyvinyl toluene block made of CaF_2:Eu phosphor (Saint-Gobain Crystals, Hiram, OH, USA). CaF_2:Eu was selected as the optimal scintillating materials with respect to highest radioluminescent signal[25]. The phosphor has a refractive index of 1.58 with 68% light output. The scintillating efficiency was 10,400 photons/1 MeV e-. It has a maximum emission at 435

nm wavelength with a temporal pulse width of 2.2 ns (FWHM). The scintillating window was machined into a cylindrically shaped tube with 10 mm length and wall thickness of 0.150 mm. The outer diameter (OD) and inner diameter (ID) of the window is 2.31 mm and 2.01 mm, respectively. Radioluminescence is produced within the scintillating imaging window following the emission of a beta particle from a radiotracer (^{18}F-FDG) within a macrophage. The optical photons were captured by a high-numerical-aperture 10x microscope objective coupled to a deep-cooled ProEM CCD camera. This scintillating window can detect radioluminescent signal from the disease tissue within the travel distance of β-particles (1-3 mm in tissue) emitted from the ^{18}F-FDG decay. The CRI peripheral system provides the overall spatial resolution of the CIRPI system that is 1.2 μm based on our previous study[25]. Spatial resolution of the CRI was calculated based on modulation transfer function (MTF). MTF is an important aid to objective evaluation of the image-forming capability of our CRI peripheral system, providing a means of expressing the imaging quality of the optical system objectively and quantitatively, plus predicting performance reliably. The detection limit and overall radioluminescence signal sensitivity of our system was identified to be 10,020 (photon counts) based on a 1 μCi closed disk β-source.

Circumferential sector scanning (B-scan) was accomplished by rotating a 45˚ flat mirror. The mirror was driven by a geared actuator (gear ratio, 254:1) to steer the laser beam from the optical fiber to the tissue and the acoustic wave from the tissue to the ultrasonic transducer (UST). A single 360º arterial PAT image acquisition time is 1.15 seconds for our CIRPI system. Therefore, the overall detection speed for a 360˚ view of an artery with our CIRPI system took only few minutes (≈2 minutes). When the pulsed laser light illuminated atherosclerotic plaque, the optical absorbers there (such as lipid, cholesterol, calcification) undergo thermo elastic expansion, generating an acoustic

pressure wave which was detected with the UST. The mirror was also important for reflecting visible light to the OF-2 due to the vibration of molecules within the scintillating imaging window upon the deposition of β-particles energy from the ^{18}F-FDG decay. As water and glass have a large ratio of sound propagation speeds, the scanning mirror has exhibited total external reflection within the acceptance angles of the ultrasonic transducer and the GRIN lens, and thus, contributed to no additional propagation losses into the ultrasonic and visible light detection. The scanning mirror system had enabled circumferential B-scanning without moving other illumination optics and the ultrasonic sensor. The optical fibers, the transducer's signal wires, and the actuator wires were encapsulated in a flexible catheter body with outer diameter of 2.31 mm where 0.5 mm was used for a catheter enclosure. The mirror's rotational speed was kept constant, while providing a matching medium for acoustic wave propagation, the transducer and scanning mirror's housing space was water-coupled with deionized water through a 0.25 mm hole on the 0.180 mm thick scintillating imaging window. The actuator was isolated from the water with a spacer, and the torque was required for the mirror rotation that is transferred through a micro-magnetic (OD 1.58 mm with a length of 3.175 mm, K&J Magnets Inc., USA) coupling mechanism.

PAT Image Reconstruction

PAT images are created from the generation of thermoelastic stress waves by heating endogenous chromophores (e.g., calcification, cholesterol) or exogenous contrast agents in an optically heterogenous medium with a short laser pulse. These stress waves contain information about the distribution of structures with preferential optical absorption. Therefore, information about the relative concentrations of endogenous chromophores or exogenous contrast agents can be determined allowing

enhanced signal to background ratios. The low optical absorption and US scattering of disease tissues makes it optimal for PAT imaging at high resolution and depth (maximum 3-5 cm deep). However, for this study we adjusted the depth to be between 5-8 mm.

The temporarily confined optical absorption induces a temperature rise ΔT and consequently an initial pressure rise p_0 due to thermoelastic expansion: $p_0 = \beta . \Delta T/k$, where k is the isothermal compressibility. The PA signal was collected every 1.43º rotating step of the scanning mirror for photoacoustic acquisition at seven different wavelengths. The PAT image was developed one laser pulse per image line. The procedure of PA signal processing includes high-pass signal filtering, compensation for acoustic diffraction, detection of the irradiated surface position and rejection of the reverberating signal. Radial back-projection algorithm for image reconstruction was developed and included in the Labview/Matlab computer code. Laser induced noise was removed with singular value decomposition method.

Co-Registered with Histological Analyses and OCT

After the in vivo imaging experiments, WHHL (n=5) and NZW (n=2) rabbit dorsal abdominal aortic samples were cut from the distal edge of the stent (used as a landmark) and placed in 10% formalin, and submitted for paraffin embedding, sectioning, and staining. Step sections (5 µm thick, n=16) were collected at different levels beginning at the proximal end of the stent to exclude the aorta containing stent (otherwise blade would brake) and proceeding to the other end. The sections were mounted on glass microscopic slides, stained with hemotoxylin and eosin, trichrome (collagen), and EVG (elastin) reagents and covered with Tissue Tek Film as cover slips.

The microscopic slides were examined with an Olympus BX51 microscope fitted with diffuse white light (LM) and transmission polarizing (TPM) optics and 2x, 4x, 10x,

20x, and 40x objectives. Selected fields were imaged by pathologist at Stanford SOM using Zeiss Axiocam MRc5 digital camera mounted on the microscope and Zeiss AxioVision SE64 Rel 4.8 software supported by a Dell Optiplex 980 Desktop Computer. The histological study was based on a quantitative analysis of disease tissue constituents that were co-register with the CIRPI results and clinical OCT based on the stent location.

Safety Assurance

After each experiment, we used classical gamma counting analog meter, Geiger-Muller counter, to perform safety assurance on the instruments, counter top, whole body, and lab coat, that there was no contamination from ^{18}F-FDG. Each time the count per minute was around 30-50 CPM that was in normal range of 0.03-0.05 mR/hr.

Statistical Analysis

A pairwise two-sample Student's t-test was performed to compare *in vivo* radioluminescent signal intensity from the ^{18}F-FDG-enriched vulnerable plaques and stable plaques. The same t-test was performed for PA signals as well for both TCFA and non-TCFA. As WHHL rabbits had similar weight (5±0.02lb) and same dose, these factors were not considered in the statistical analysis. Therefore, weight and dose were eliminated during the statistical process. Rabbit samples were not randomized. These analyses were performed using custom written MATLAB code. We presented all values as mean ± standard deviation. We considered $P<0.05$ as statistically significant for all ex vivo analyses.

For a significance level of $P<0.05$ and a statistical power of 0.90, each group should comprise of at least N=5 animals to obtain a statistically significant result. We used an equation for sample size calculation for a study comparing two means:

$N=\{4*\sigma^2(Z_{crit}+Z_{pwr})^2\}/D^2$ where N is sample size, D is the minimum expected CNR difference based on the means of the two groups (plaque vs. control), σ is assumed standard deviation of each group (assumed to be equal for both group) be 1.65, Z_{crit} = 1.960 for significance level of 0.05(95) (standard normal deviate corresponding to selected significance criteria) and Z_{pwr} = 1.645 for statistical power of 0.95 (standard normal deviate corresponding to selected statistical powers) .

Supplemental Table 1. Observations of In Vivo Rabbit Samples with CIRPI, OCT, and Histochemical Analysis

Species	**Observation**		
Rabbit ID	**CIRPI Image Analysis**	**OCT Image Analysis**	**Histochemical Analysis**
# R317 Gender: Male Age: 13 months (Disease WHHL rabbit)	1. Moderate macrophages 2. No calcification 3. No cholesterol clefts in the forms of cholesterol ester, phospholipids, cholesterol, and triglyceride 4. Presence of intact elastic fibers and collagen	1. Only intimal hypertrophy 2. Early stage atherosclerosis 3. No lipid filled TCFA plaques 4. Early stage plaques are developing 17.1 mm away from proximal stent edge (PSE)	1. 10% or less occlusion 2. Near the PSE showed macrophage accumulation and thrombus 3. No mineralized calcium 4. No lipid/cholesterol 5. 500 µm plaque area 6. Small amounts of collagen deposition and presence of intact elastic fiber
# R417 Gender: Male Age: 13 months (Disease WHHL rabbit)	1. Moderate macrophages 2. Moderate calcification 3. Presence of severe cholesterol cleft in forms of cholesterol ester, phospholipids, cholesterol, and triglyceride 4. Presence of broken elastic fibers and collagen	1. TCFA (wall thickness 65 µm) starts from 7.9 mm from PSE 2. Continuous plaques in the entire length of the vessel wall 3. One side of the vessel wall is normal thickness while the other end of the wall is developing plaques with Narrowing of the vessel diameter	1. 30% lumen occlusion 2. Moderate macrophages 3. Moderate mineralized calcium 4. Moderate cholesterol and lipid deposition 5. Moderate inflammation 6. 600 µm plaque area 7. Presence of broken elastic fibers and collagen
# R517 Gender: Male Age: 13 months (Disease WHHL rabbit)	1. Sparse macrophages 2. Moderate calcification 3. Severe cholesterol clefts in forms of cholesterol ester, phospholipids, cholesterol, and triglyceride 4. Presence of broken elastic fibers and collagen	1. TCFA started from 14.1 mm away from PSE 2. Lipid filled plaques with 40 µm wall thickness 3. Most stable plaques were between the PSE and TCFA	1. 25% lumen occlusion 2. Moderate macrophages 3. Moderate mineralized calcium 4. Severe lipid/giant cells with moderate cholesterol formation 5. Moderate chronic inflammation 6. 750 µm plaque area 7. Presence of broken elastic fibers and collagen
# R617 Gender: Male Age: 13 months (Disease WHHL rabbit)	1. Severe macrophages 2. Severe calcification 3. Severe cholesterol ester, phospholipids, cholesterol, and triglyceride 4. Presence of broken elastic fibers and collagen	1. Intimal hypertrophy 2. Both TCFA and stable plaques are present 3. Presence of multiple TCFA and stable plaques • 1st TCFA: 40 µm wall thickness (10 mm away from the PSE) • 2nd TCFA (at the end): 50 µm wall thickness (14.7 mm away from PSE) • Stable plaque: 180 µm wall thickness) (32.8 mm away from PSE)	1. 60% lumen occlusion 2. Severe macrophages 3. Severe mineralized calcium 4. Minimal inflammation 5. Severe cholesterol clefts and lipid deposition 6. 500 µm plaque area 7. Presence of broken elastic fibers and collagen

# R717 Gender: Male Age: 13 months (Disease WHHL rabbit)	1. Sparse macrophages 2. Severe calcification 3. Severe cholesterol ester, phospholipids, cholesterol, and triglyceride 4. Presence of broken elastic fibers and collagen	1. Intimal hypertrophy 2. Mostly early stage atherosclerosis with few TCFA and stable plaques 3. TCFA with a wall thickness of 60 μm is located 30.9 mm away from PSE 4. Mostly stable plaques from PSE up to 30.9 mm where the TCFA started	1. 45% lumen occlusion 2. Sparse macrophages 3. Severe mineralized calcium 1. 500 μm plaque area with 1 mm length 2. Calcification 3. Macrophages or histocytes 4. Cholesterol cleft 5. Broken elastic fiber
# R817/R917 Gender: Male Age: 13 months (Control NZW rabbit)	1. No macrophages 2. No calcification 3. No cholesterol cleft 4. Presence of intact elastic fibers and collagen	1. No atherosclerotic plaques 2. Normal wall thickness	1. No evidence of atherosclerotic plaques, calcification, cholesterol, or macrophages 2. Normal wall thickness 3. Presence of intact elastic fibers and collagen

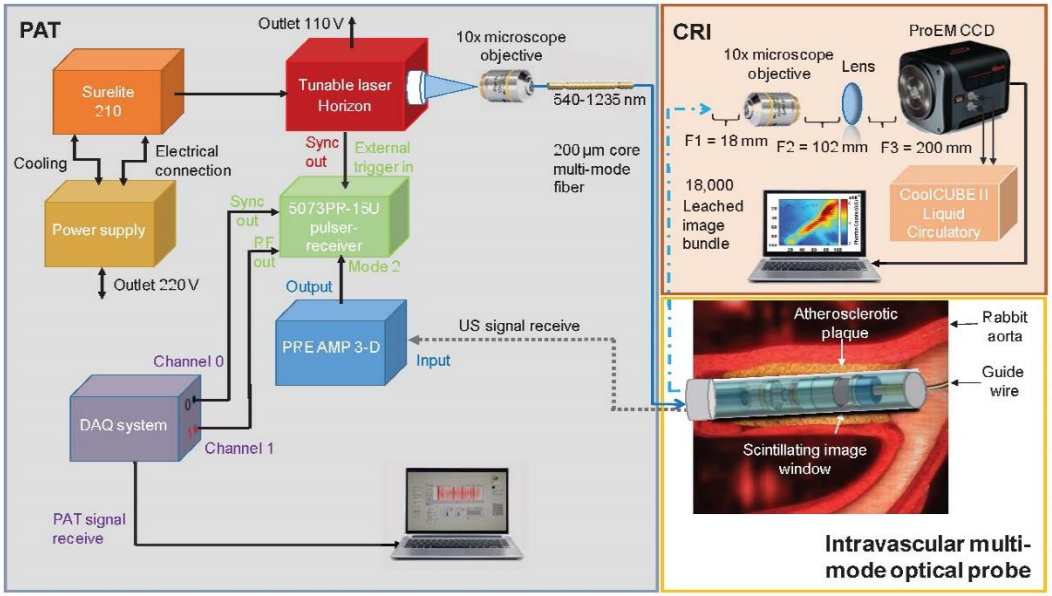

Supplemental Fig 1. Schematic diagram of the dual-modality CIRPI system for detection and characterization of atherosclerotic plaque. The CIRPI system has three main components (1) CRI, detects and outlines the location of vulnerable plaque by identifying macrophage accumulations, (2) PAT, characterize the plaque by disease tissue compositions, and (3) multi-mode optical probe that collects radioluminescent and PA signals. CRI peripheral system consists of (1) a 10x magnification infinity-corrected microscope objective (2) an infinity-corrected tube lens for plan fluoride objective in between the objective (F2 = 102 mm) and the ProEM charge-coupled device (CCD) camera (F3 = 200 mm). PAT system consists of (1) tunable laser, (2) pulser-receiver, (3) pre-amplifier, (4) data acquisition board (DAQ system).

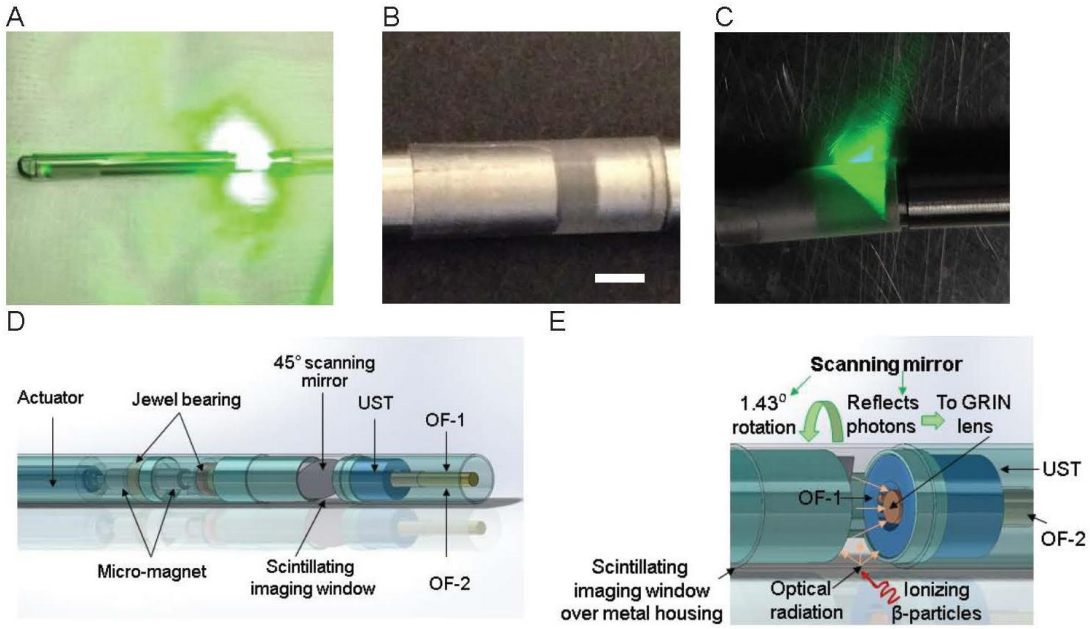

Supplemental Fig 2. Photograph of the (A) multi-mode optical probe with scintillating imaging window (B) scintillating imaging window is made from CaF_2:Eu phosphor (scale bar: 1 mm) that converts beta particles to visible photons, (C) tunable laser light is delivered through water coupled scintillating window at 540 nm (Visible, green), 560 nm (Visible, green), and 1040 nm wavelength (NIR, Near InfraRed). Schematic diagram of the CIRPI (D) probe design shows the main components (1) CaF_2:Eu scintillating imaging window, (2) OF-1: 0.2 mm core multimode light guiding optical fiber, (3) OF-2: 18K pixels imaging fiber, (4) UST: single element unfocused ultrasonic transducer, (5) digital actuator, and (6) 45° degree flat rotating mirror, (E) optical pathway of the visible photons reflecting from the scanning mirror to the GRIN lens at every 1.43º rotation and facilitating a single radioluminescence image with 18,000 pixels through OF-2.

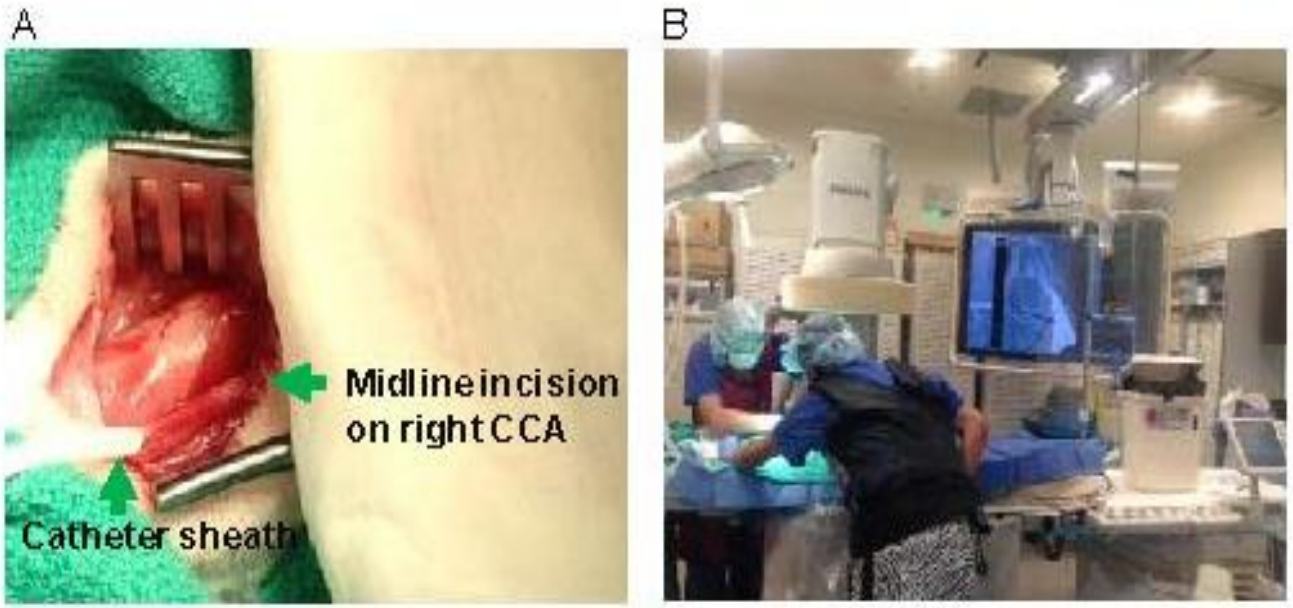

Supplemental Fig 3. In vivo rabbit expertiental procedure. (A) A catheter sheath is inserted throught a midline incision on the right CCA after the tissue was separted and hold with a speculum. (A) Interventional cardiologist is inserting the imaging catheter with a guide wire through a midline incision on either the right/left CCA guiding through a X-ray fluoroscopy in a surgical suite.

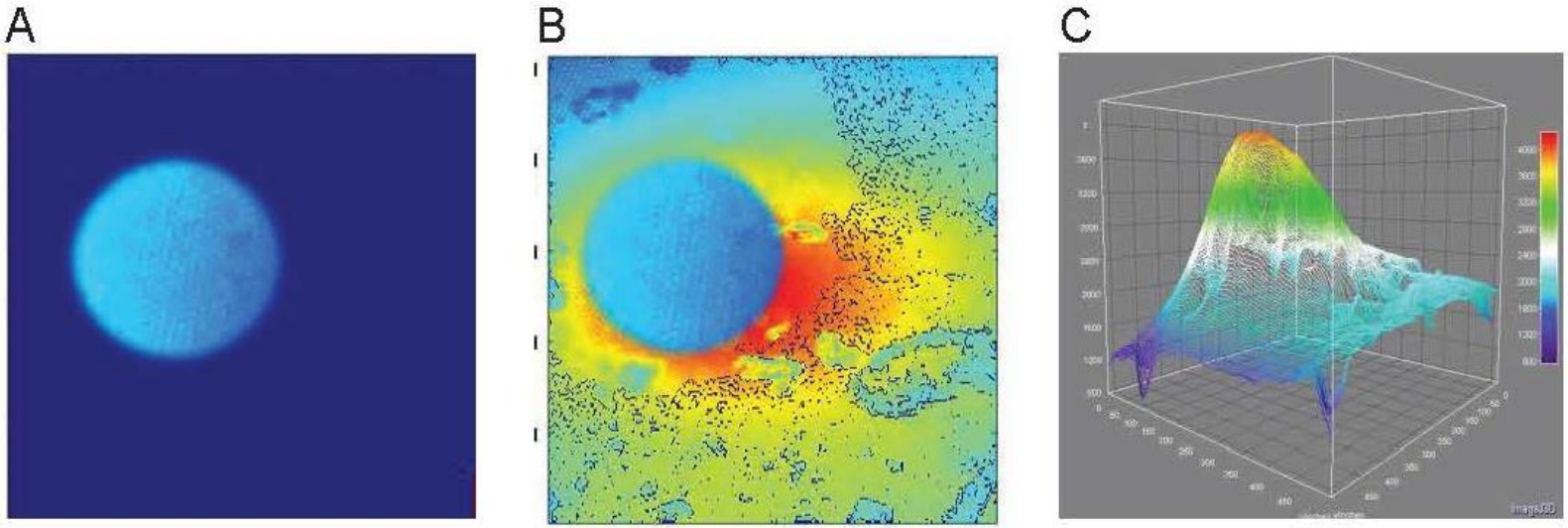

Supplemental Fig 4. A reconstructed radioluminescence image of a 360º arterial view (A) control rabbit, (B) disease rabbit. (C) Contour plot of the diseased rabbit.